CONFIDENTIAL

Copy
RM E54D21

NACA RM E54D21

NACA

RESEARCH MEMORANDUM

ANALYSIS OF FACTORS AFFECTING SELECTION AND DESIGN OF AIR-COOLED SINGLE-STAGE TURBINES FOR TURBOJET ENGINES

II - ANALYTICAL TECHNIQUES

By Richard J. Rossbach

Lewis Flight Propulsion Laboratory
Cleveland, Ohio

This material contains information affecting the National Defense of the United States within the meaning of the espionage laws, Title 18, U.S.C., Secs. 793 and 794, the transmission or revelation of which in any manner to an unauthorized person is prohibited by law.

NATIONAL ADVISORY COMMITTEE
FOR AERONAUTICS

WASHINGTON
June 21, 1954

CONFIDENTIAL

NACA RM E54D21

NATIONAL ADVISORY COMMITTEE FOR AERONAUTICS

RESEARCH MEMORANDUM

ANALYSIS OF FACTORS AFFECTING SELECTION AND DESIGN OF AIR-COOLED SINGLE-STAGE TURBINES FOR TURBOJET ENGINES

II - ANALYTICAL TECHNIQUES

By Richard J. Rossbach

SUMMARY

In order to obtain a better understanding of the potential air-cooled turbojet-engine performance, studies are required to investigate both the engine-performance capabilities and the effect of losses associated with turbine air-cooling on engine performance. This report presents computational methods for analyzing turbojet-engine performance for a series of air-cooled nonafterburning and afterburning engines where all the engine components are simultaneously aerodynamically limited. The coolant-flow ratio was arbitrarily assigned so that the results of the analysis can be applied to any specific air-cooled blade configuration. The work required to compress the cooling air, the drag of the cooling air upon the turbine, the losses which occur when the cooling air and the combustion gases mix downstream of the turbine, and losses in the combustor and afterburner are taken into account. Techniques are also presented for determining the relative frontal areas of the various engine components.

INTRODUCTION

The design and performance of the turbojet engine are, to a great degree, controlled by the turbine component, which in conventional engines limits the turbine-inlet temperature and in many cases the mass weight-flow capacity due to stress-limited turbine annulus area. By use of turbine cooling, the blade temperature and blade strength can be controlled independent of the turbine-inlet temperature, with the result that greater ranges in turbine and engine operation are possible. In order to explore the range of engine operation that can be made possible through use of turbine cooling, analytical techniques are developed herein to determine the design performance of single-stage air-cooled turbines operating over wide ranges of turbine design specifications. This turbine performance is then used to evaluate potential engine design performance for both nonafterburning and afterburning engines.

Previous analytical studies on the engine performance obtainable by utilizing turbine cooling are cited in reference 1, and the effect of air-cooling on performance of existing engines is reported in references 2 and 3. In all previous investigations, however, no consideration was given to the beneficial effects of higher turbine-inlet temperatures and turbine-blade stresses on the turbine work and engine weight-flow capacity. A recent publication (ref. 4) provides a simplified procedure for determining the turbine specific work for a given combination of the turbine design specifications (i.e., turbine-inlet temperature, turbine-blade tip speed, and turbine-blade hub-tip radius ratio). With this procedure, it is possible to analyze within a reasonable length of time a large number of turbines, as would be required for evaluating the design performances of turbojet engines over wide ranges of design conditions. In addition, recent component research permits good estimates of the component efficiencies and aerodynamic limits as needed for accurate evaluation of component losses and weight-flow capacity. Therefore, a series of investigations has been undertaken by the NACA Lewis laboratory to determine the design performances of turbojet engines over a wide range of operating conditions; these investigations employ an aerothermodynamic analysis which uses the maximum obtainable turbine work within established design limitations and relates the engine weight flow to the weight-flow capacity of the engine components. The turbine design specifications are utilized as the independent variables, since along with the component aerodynamic limits and efficiencies they adequately specify the turbine-cooling requirements as well as the requirements necessary for computing the engine performance. The analysis permits computation of values of the engine specific weight flows and compressor pressure ratios which are compatible and assures realistic turbine designs and comparable engines.

The first part of this investigation is reported in reference 1, which presents the turbine design performance (in terms of the obtainable compressor pressure ratio and turbine weight flow) and the engine weight-flow capacity for nonafterburning and afterburning engines equipped with air-cooled single-stage turbines and operating with high component aerodynamic limits. The purpose of the present report is to present the analytical techniques required to obtain the turbine design performance, engine weight-flow capacity, and over-all engine design performance. In the interest of providing results suitable for any specific air-cooled blade configuration, the analytical techniques are set up to employ a range of cooling air flow rather than the cooling air flow required for a single air-cooled blade configuration. The analysis also permits the determination of all stagnation temperatures and pressures within the engine and the ratio of all component frontal areas.

ASSUMPTIONS

The following assumptions were made to facilitate the analysis:

(1) Inasmuch as the condition of simplified radial equilibrium was imposed upon the turbines of reference 4 and was suggested in reference 5 as a means of obtaining the first approximation to the conditions in a compressor, this condition was imposed upon the analysis of the turbine and the inlet to the compressor.

(2) The turbine was analyzed on the basis of free-vortex blading (ref. 4).

(3) Solid-body-rotation guide vanes were employed in the analysis of the compressor inlet.

(4) The density at the mean radial position was employed for computing the weight flow through the turbine (ref. 4) and the compressor inlet.

(5) The stagnation temperature was considered invariant with the radial position at the entrances to the turbine (ref. 4) and the compressor.

(6) The hub, mean, and tip radii at the turbine exit were considered equal to the respective values at the entrance to the turbine (ref. 4).

(7) A constant value of 4/3 for the ratio of specific heats was employed in the analysis of the combustor and turbine (ref. 4).

(8) The analysis was made on the basis of adiabatic flow through the turbine.

(9) The work done by the turbine upon the cooling air between the compressor entrance and the tips of the turbine blades was considered equivalent to the work required to compress the cooling air to the compressor-discharge stagnation temperature.

(10) The mechanical friction and the work required by accessories were considered to be negligible in the analysis of the turbine.

(11) The pressure head associated with the tangential component of the turbine absolute efflux velocity was considered to be dissipated by the struts which secure the tail cone, and the loss was charged to the adiabatic efficiency.

(12) Upon the basis of some unpublished data obtained by the NACA and the results presented in reference 6, the efflux of the cooling air from the tips of the turbine blades was considered not to affect the turbine specific work or adiabatic efficiency.

(13) The pressure ratio of the combustor was varied with the inlet Mach number and the temperature ratio according to the experimental loss characteristics of the typical low-loss turbojet combustor studied in reference 7.

(14) The combustion gases and the cooling air were considered to enter the zone in which mixing occurred downstream of the turbine at the same static pressure.

(15) The flow area in the mixing zone for the turbine exhaust gases and the cooling air was considered constant.

(16) As in reference 8, the afterburner was considered to have a constant-area combustion section.

(17) In the afterburner, the friction and flame-holder losses were assumed to be given by a constant times the inlet dynamic head as in reference 8.

(18) In computing the thrust, complete expansion to the ambient pressure was assumed, because, as shown in reference 9, such an expansion results in the maximum thrust at the flight Mach numbers of 2 and higher.

In the figures presented herein, as well as in reference 1, the following values of the constants were employed:

$$B = 5.5$$

$$E = 4.5$$

$$G = 3.0$$

$$M_{R,2,t} = 1.1$$

$$M_{R,5,h} = 0.8$$

$$\frac{r_{B,h}}{r_t} = 0.25$$

$$T_2' = 708^\circ \text{ R}$$

$$\frac{V_{x,2,h}}{a_2^*} = 0.7$$

$$\frac{V_{x,6}}{a_6^*} = 0.7$$

[redacted]

$$\frac{V_{u,6,i}}{U_i} = -0.410$$

$$\eta_C = 0.83$$

$$\eta_T = 0.83$$

The symbols used in this report are defined in the appendix, and the schematic diagrams of the nonafterburning and afterburning engines are presented in figure 1.

ANALYTICAL TECHNIQUES

The independent variables chosen for this analysis are the turbine design specifications: turbine-inlet temperature, tip speed, the hub-tip radius ratio of the turbine, and arbitrary values of the coolant-flow ratio. The employment of the latter variable facilitates specializing the results to any cooled-blade configuration. In order to relate the engine design performance to the turbine design specifications and the coolant-flow ratio, it is necessary to impose aerodynamic limits upon each of the engine components in addition to and commensurate with its respective efficiency.

The performance analysis is initiated with the turbine component; this component limits the output of the engine through the control it exercises over the weight flow of the engine and the pressure ratio of the compressor. Both the weight flow and the compressor pressure ratio determined are the maximum values obtainable from a single-stage, air-cooled turbine having the values of the aerodynamic limits assigned. The attainment of high compressor pressure ratio and engine weight flow are emphasized in this analysis so that the highest engine performance is attained for the least value of coolant-flow ratio.

Compressor pressure ratio. - The compressor pressure ratio for a given compressor-inlet temperature and adiabatic efficiency depends upon the turbine specific work. In reference 4 (eq. (E1)), the turbine specific work is expressed in the form of Euler's turbine equation as

$$-g\frac{J\Delta h_T'}{U_t^2} = \frac{V_{u,5,t}}{U_t} - \frac{V_{u,6,t}}{U_t} \tag{1}$$

The value of the exit whirl can be conveniently specified by the ratio of whirl component of velocity to wheel speed $V_{u,6,i}/U_i$ at the radial position at which the product of whirl-energy loss per pound and total weight flow expresses the total whirl loss. Upon integrating the whirl-energy loss over the blade height, it can be shown that the value of $V_{u,6,t}/U_t$ used in equation (1) is related to $V_{u,6,i}/U_i$ by the expression

[redacted]

$$\frac{V_{u,6,t}}{U_t} = \frac{V_{u,6,i}}{U_i}\left(\frac{r_i}{r_t}\right)^2 = \frac{V_{u,6,i}}{U_i}\left[\frac{1 - \left(\frac{r_h}{r_t}\right)^2}{\ln\left(\frac{r_t}{r_h}\right)^2}\right] \tag{2}$$

It can be shown that $V_{u,5,t}/U_t$, as required in equation (1), is given by the functional relation

$$\frac{V_{u,5,t}}{U_t} = fn\left(M_{R,5,h}, \frac{V_{x,6}}{a_6^*}, \frac{V_{u,6,t}}{a_6^*}, \eta_T, \frac{U_t}{a_6^*}, \frac{r_h}{r_t}\right) \tag{3}$$

where $M_{R,5,h}$ and $V_{x,6}/a_6^*$ are the turbine aerodynamic limits. Charts for solving equation (3) for $V_{u,6,t}/a_6^* = 0$ are presented in reference 4. Since $V_{u,6,t}/a_6^*$ has a small effect on the value of $V_{u,5,t}/U_t$ for aerodynamically limited turbine designs (ref. 4), the chart of reference 4 can be employed to solve for $V_{u,5,t}/U_t$ if $V_{u,6,t}/a_6^*$ is assumed to be zero.

The following equations, which employ the values of $V_{u,5,t}/U_t$ and $V_{u,6,t}/U_t$, were used to obtain figure 2 and to determine the turbine temperature ratio:

$$\frac{T_6'}{T_4'} = \left[1 + 2\left(\frac{\gamma-1}{\gamma+1}\right)\left(\frac{U_t}{a_6^*}\right)^2\left(\frac{V_{u,5,t}}{U_t} - \frac{V_{u,6,t}}{U_t}\right)\right]^{-1} \tag{4}$$

$$\frac{U_t}{a_4^*} = \frac{U_t}{a_6^*}\sqrt{\frac{T_6'}{T_4'}} \tag{5}$$

Equation (4) was obtained from equation (1) and the energy equation in terms of turbine-inlet and -exit temperature. Since

$$a_4^* = \sqrt{\frac{2\gamma g R T_4'}{\gamma+1}}$$

figure 2 was employed to obtain a unique value of T_6' for each set of values of T_4', U_t, and r_h/r_t. The turbine specific work was then obtained from

$$\Delta h_T' = \frac{-R}{J}\frac{\gamma}{\gamma-1}(T_4' - T_6') \tag{6}$$

3308

The work and weight-flow balances on the compressor and turbine lead to

$$(1 - C)\,\Delta h_T' = \frac{-\Delta h_C'}{(1 + f_B)} \tag{7}$$

The right side of equation (7) can be expressed as a function of the compressor pressure ratio and the turbine-inlet temperature by means of the charts and methods of reference 10. The left side of equation (7) is plotted against the compressor pressure ratio with the turbine-inlet temperature as a parameter in figure 3. Byproducts of these calculations are the compressor-outlet temperature and the combustor fuel-air ratio, which are presented in figures 4 and 5, respectively. Since the turbine specific work is given by equation (6), the compressor pressure ratio, the compressor-outlet temperature, and the fuel-air ratio can be obtained from figures 3 to 5 for an assigned value of the coolant-flow ratio.

Compressor specific weight flow. - The compressor specific weight flow is computed from the following form of the continuity equation:

$$\frac{w_C\sqrt{\theta_2}}{A_C\delta_2} = p_0\sqrt{\frac{2\gamma_2 g}{(\gamma_2 + 1)RT_0}}\left(\frac{V_{x,2,m}}{a_2^*}\right)\left[1 - \frac{\gamma_2 - 1}{\gamma_2 + 1}\left(\frac{V_{2,m}}{a_2^*}\right)^2\right]^{\frac{1}{\gamma_2 - 1}}\left[1 - \left(\frac{r_h}{r_t}\right)_C^2\right] \tag{8}$$

The solution of equation (8) depends upon the following equations developed from the condition of simplified radial equilibrium (assumption (1)), the condition of solid-body rotation (assumption (3)), and the condition of constant-energy flow:

$$\left(\frac{V_{2,m}}{a_2^*}\right)^2 = \left(\frac{V_{2,t}}{a_2^*}\right)^2 + \left[1 - \left(\frac{r_m}{r_t}\right)_C^2\right]\left(\frac{V_{u,2,t}}{a_2^*}\right)^2 \tag{9}$$

and

$$\left(\frac{V_{x,2,m}}{a_2^*}\right)^2 = \left(\frac{V_{2,t}}{a_2^*}\right)^2 + \left[1 - 2\left(\frac{r_m}{r_t}\right)_C^2\right]\left(\frac{V_{u,2,t}}{a_2^*}\right)^2 \tag{10}$$

Other equations required for the solution of equation (8) are the following:

$$\frac{V_{u,2,t}}{a^*_2} = \frac{\left(\frac{U_t}{a^*_2}\right)^2 + \left(\frac{V_{2,t}}{a^*_2}\right)^2 - \left(\frac{W_{2,t}}{a^*_2}\right)^2}{2\left(\frac{U_t}{a^*_2}\right)} \tag{11}$$

and

$$\left(\frac{W_{2,t}}{a^*_2}\right)^2 = \frac{\gamma_2+1}{2}\left(M_{R,2,t}\right)^2\left[1 - \frac{\gamma_2-1}{\gamma_2+1}\left(\frac{V_{2,t}}{a^*_2}\right)^2\right] \tag{12}$$

$$\frac{V_{2,t}}{a^*_2} = \left[\frac{-K_1 + \sqrt{K_1^2 - 4K_2}}{2}\right]^{1/2} \tag{13}$$

in which

$$K_1 = \frac{\left[2\left(\frac{U_t}{a^*_2}\right)^2 - \frac{\gamma_2+1}{2}\left(M_{R,2,t}\right)^2\right]}{\left[1 + \frac{\gamma_2-1}{2}\left(M_{R,2,t}\right)^2\right]} + \frac{4\left(\frac{U_t}{a^*_2}\right)^2}{\left[1 - 2\left(\frac{r_h}{r_t}\right)^2_c\right]\left[1 + \frac{\gamma_2-1}{2}\left(M_{R,2,t}\right)^2\right]} \tag{14}$$

and

$$K_2 = \frac{\left[\left(\frac{U_t}{a^*_2}\right)^2 - \frac{\gamma_2+1}{2}\left(M_{R,2,t}\right)^2\right]^2}{\left[1 + \frac{\gamma_2-1}{2}\left(M_{R,2,t}\right)^2\right]^2} - \frac{4\left(\frac{V_{x,2,h}}{a^*_2}\right)^2\left(\frac{U_t}{a^*_2}\right)^2}{\left[1 - 2\left(\frac{r_h}{r_t}\right)^2_c\right]\left[1 + \frac{\gamma_2-1}{2}\left(M_{R,2,t}\right)^2\right]^2} \tag{15}$$

The preceding equations were obtained from the application of the Pythagorean theorem to the hub velocity-vector diagram and the law of cosines to the tip velocity-vector diagram, the definition of the inlet relative Mach number at the hub, the condition of solid-body rotation, and the expression for the spanwise absolute inlet velocity distribution. In the solution of the equations for the compressor specific weight flow, values are assigned for the rotor-inlet tip relative Mach number, the inlet axial critical velocity ratio, and the compressor hub-tip radius ratio.

[redacted]

Degree of reaction. - A static-pressure rise through a turbine rotor (negative reaction) at any spanwise position is likely to cause flow separation. In the case of a free-vortex turbine design, the reaction decreases from tip to hub. In reference 4, it is pointed out that for a real turbine, that is, for one having losses, a condition which is slightly more conservative than a limit of zero reaction is the condition in which the magnitude of the relative velocity at the hub is at least as large at the exit as at the entrance. The following equation, which contains the conditions of a limited inlet relative hub Mach number and zero change in the magnitude of the relative velocity across the hub of the rotor, permits the determination of the lowest value of U_t/a_6^* for a given set of turbine design specifications for which the reaction at the hub is positive:

$$\left(\frac{U_t}{a_6^*}\right)^2_{\frac{W_{5,h}}{W_{6,h}}=1} = \frac{\left\{\frac{\gamma+1}{2}\left(M_{R,5,h}\right)^2 - \left(\frac{V_{x,6}}{a^*}\right)\left[1+\frac{\gamma-1}{2}\left(M_{R,5,h}\right)^2\right]\right\}}{\left(\frac{r_h}{r_t}\right)^2\left\{\left[1+\frac{\gamma-1}{2}\left(M_{R,5,h}\right)^2\right]\left(\frac{V_{u,6,h}}{U_h}-1\right)^2 - \frac{\gamma-1}{2}\left(M_{R,5,h}\right)^2\right\}} \tag{16}$$

Equation (16) was employed to plot the dashed line in figure 2.

Turbine-limited specific weight flow. - The turbine weight flow per unit turbine frontal area is determined at the turbine exit from the continuity equation in the form

$$\frac{w_T}{A_T} = \frac{p_6' a_6^*}{RT_6'}\left(\frac{V_{x,6}}{a_6^*}\right)\left[1-\frac{\gamma-1}{\gamma+1}\left(\frac{V_{x,6}/a_6^*}{\sin\alpha_{6,m}}\right)^2\right]^{\frac{1}{\gamma-1}}\left[1-\left(\frac{r_h}{r_t}\right)^2\right] \tag{17}$$

in which

$$\sin^2\alpha_{6,m} = \tan^2\alpha_{6,m}/\left(1+\tan^2\alpha_{6,m}\right) \tag{18}$$

and

$$\tan\alpha_{6,m} = \left(\frac{V_{x,6}}{a_6^*}\,\frac{U_t}{V_{u,6,t}}\,\frac{1+r_h/r_t}{2}\,\frac{a_6^*}{U_t}\right) \tag{19}$$

In order to solve equation (17), the assigned value of the exit axial critical velocity ratio is employed and all the component pressure ratios from the inlet diffuser through the turbine must be determined.

[redacted]

The inlet diffuser pressure ratio, resulting from the isentropic relation and the definition of the ram recovery, is given by

$$\frac{p_2'}{p_\infty} = \eta_R \left(1 + \frac{\gamma_\infty - 1}{2} M_\infty^2\right)^{\frac{\gamma_\infty}{\gamma_\infty - 1}} \tag{20}$$

In equation (20), the flight condition and the ram recovery are assigned. The compressor pressure ratio is determined from figure 3.

In order to obtain the combustor pressure ratio for the case in which the combustor reference velocity (combustor weight flow divided by the product of the largest cross section and the combustor-inlet density) is limited, the momentum and continuity relations must be solved simultaneously. The useful form of the momentum equation is given by

$$\frac{p_4'}{p_3'} = \frac{1}{2}\left[\left(1 - \frac{B}{2gR}\frac{V_B^2}{T_3'}\right) + \sqrt{\left(1 - \frac{B}{2gR}\frac{V_B^2}{T_3'}\right)^2 - \frac{2E}{gR}\frac{V_B^2}{T_3'}\frac{T_4'}{T_3'}}\right] \tag{21}$$

Employing w_T/A_T as given by equation (17) results in the following useful form of the continuity equation:

$$\frac{p_4'}{p_3'} = S\left\{\left[\frac{1 - \frac{\gamma-1}{2}\left(\frac{G^2}{\gamma gR}\right)\frac{V_B^2}{T_3'}}{1 - \frac{\gamma-1}{\gamma+1}\left(\frac{V_{x,6}}{a_6^*}\right)^2}\right]^{\frac{1}{\gamma-1}} \frac{\frac{V_B}{\sqrt{T_3'}}}{\frac{V_{x,6}}{a_6^*}}\right\} \tag{22}$$

in which

$$S = \frac{\sqrt{\frac{\gamma+1}{2\gamma gR}\frac{T_6'}{T_3'}}\left[\left(\frac{r_{B,t}}{r_t}\right)^2 - \left(\frac{r_{B,h}}{r_t}\right)^2\right]}{\frac{p_6'}{p_4'}\left[1 - \left(\frac{r_h}{r_t}\right)^2\right]}\left[\frac{1 - \frac{\gamma-1}{\gamma+1}\left(\frac{V_{x,6}}{a_6^*}\right)^2}{1 - \frac{\gamma-1}{\gamma+1}\left(\frac{V_{x,6}/a_6^*}{\sin\alpha_{6,m}}\right)^2}\right]^{\frac{1}{\gamma-1}} \tag{23}$$

In figure 6, equations (21) and (22) are plotted with the same ordinate and abscissa. The empirical constants B and E in equation (21) were obtained from the pressure-drop data on the typical low-loss combustor studied in reference 7. Values of 3.0 and 0.25 were assigned to the combustor-inlet diffuser-area ratio G and the combustor-inner- to the turbine-tip-radius ratio, respectively.

[redacted]

The combustor temperature ratio T'_4/T'_3, which is used as a parameter in figure 6, is computed from the specified turbine-inlet temperature and the compressor-outlet temperature. Therefore, in order to evaluate the combustor pressure ratio p'_4/p'_3 from figure 6, either V_B^2/T'_3 or S must also be known. If either V_B^2/T'_3 or S is known, a point is fixed on figure 6 and, therefore, both V_B^2/T'_3 and S as well as the combustor pressure ratio are fixed. In the event that the combustor velocity must be limited and the combustor frontal area must be at least as large as the turbine frontal area to minimize pressure losses, the following procedure for using figure 6 is suggested: (1) Evaluate S with the combustor and turbine frontal areas assumed equal ($r_{B,t}/r_t = 1.0$). (2) From this value of S and combustor temperature ratio T'_4/T'_3, determine V_B^2/T'_3 and p'_4/p'_3 from figure 6. (3) Compute V_B from this value of V_B^2/T'_3 and from the value of the compressor-outlet temperature T'_3. (4) If the computed value of V_B is equal to or less than the limiting values, use the corresponding value of p'_4/p'_3. If the computed value of V_B is greater than the limiting value, compute V_B^2/T'_3 for the limiting value and use this V_B^2/T'_3 along with T'_4/T'_3 to determine S and p'_4/p'_3.

The turbine pressure ratio is determined from the energy equation written across the turbine and corrected for exit whirl. The correction is required because the adiabatic efficiency is charged with the pressure head associated with the tangential component of the efflux velocity (assumption (11)). The equation from which the turbine stagnation-pressure ratio is obtained is

$$\frac{p'_6}{p'_4} = \left[1 - \frac{T'_4 - T'_6}{T'_4 \eta_T}\right]^{\frac{\gamma}{\gamma-1}} \left[1 + \frac{\gamma-1}{\gamma+1}\left(\frac{V_{x,6}}{a^*_6}\right)^2 (1 - \csc^2\alpha_{6,m})\right]^{-\frac{\gamma}{\gamma-1}} \tag{24}$$

Finally, the turbine-limited specific weight flow is computed from the following equation:

$$\frac{w_C}{A_T}\frac{\sqrt{\theta_2}}{\delta_2} = \frac{w_T}{A_T}\frac{\sqrt{\theta_2}/\delta_2}{(1 + f_B)(1 - C)} \tag{25}$$

Coolant and combustion gas mixing. - After the pressure head associated with the tangential component of the turbine efflux velocity is dissipated by the tail-cone struts (assumption (11)), the combustion gas

and the coolant enter the constant-area mixing zone (assumption (15)). The critical velocity ratio of the combustion gas as it enters the mixing zone can be determined from the continuity relation in the form

$$\left[1 - \frac{\gamma_7 - 1}{\gamma_7 + 1}\left(\frac{V_7}{a_7^*}\right)^2\right]^{\frac{1}{\gamma_7 - 1}} \left(\frac{V_7}{a_7^*}\right) = \frac{\frac{RT_7'}{p_7' a_7^*}\frac{w_T}{A_T}}{\left[1 - \left(\frac{r_h}{r_t}\right)^2\right]} \tag{26}$$

and from figure 7, in which the left side of equation (26) is plotted against V_7/a_7^*. The uncorrected turbine specific weight flow from equation (17) is used in the solution of equation (26). Because the pressure head due to whirl is dissipated between stations 6 and 7 without any energy change, $T_7' = T_6'$ and $p_7' = p_{x,6}'$. To evaluate $p_{x,6}'$, the following expression for the turbine pressure ratio is used:

$$\frac{p_{x,6}'}{p_4'} = \left[1 - \frac{\left(T_4' - T_6'\right)}{T_4' \eta_T}\right]^{\frac{\gamma}{\gamma - 1}} \tag{27}$$

The specific heat ratio employed in the solution of equation (26) corresponds to f_B and T_6'. The mixture temperature is obtained from the charts of reference 10 and from the heat balance across the mixing zone in the form

$$h_8' = \frac{(1 - C)(1 + f_B)\, h_6' + C h_3'}{1 + (1 - C) f_B} \tag{28}$$

The values of enthalpy required in equation (28) can be determined from the charts of reference 10, the state conditions, and fuel-air ratio.

In order to determine the pressure ratio across the mixing zone, it is necessary to solve the momentum balance and the energy balance across the mixing zone simultaneously. State conditions of the coolant before mixing are unknown because they depend upon the cooled-blade configuration; therefore, this solution involves some approximations. However, since calculations indicated that the mixing-zone pressure ratio does not vary more than 6 percent from unity, no large error is involved. After these approximations have been made, the momentum and energy relations for the mixing zone take the form

$$\frac{p_8'}{p_7'} = \left[1 - \frac{\gamma_7 - 1}{\gamma_7 + 1}\left(\frac{V_7}{a_7^*}\right)^2\right]^{\frac{1}{\gamma_7 - 1}}\left[1 + \left(\frac{V_7}{a_7^*}\right)^2\right] \Bigg/ \left[1 - \frac{\gamma_8 - 1}{\gamma_8 + 1}\left(\frac{V_8}{a_8^*}\right)^2\right]^{\frac{1}{\gamma_8 - 1}}\left[1 + \left(\frac{V_8}{a_8^*}\right)^2\right] \tag{29}$$

$$\frac{p_8'}{p_7'} = \left[1 - \frac{\gamma_7 - 1}{\gamma_7 + 1}\left(\frac{V_7}{a_7^*}\right)^2\right]^{\frac{1}{\gamma_7 - 1}}\left[\left(\frac{V_7}{a_7^*}\right) a_7^*\right] \Bigg/ \left[1 - \frac{\gamma_8 - 1}{\gamma_8 + 1}\left(\frac{V_8}{a_8^*}\right)^2\right]^{\frac{1}{\gamma_8 - 1}}\left[\left(\frac{V_8}{a_8^*}\right) a_8^*\right] \tag{30}$$

The simultaneous solution of the preceding equations results in an expression for the critical velocity ratio after mixing in the form

$$\frac{V_8}{a_8^*} = Z_8 - \sqrt{Z_8^2 - 1} \tag{31}$$

in which

$$Z_8 = \frac{1}{2}\frac{a_8^*}{a_7^*}\left(\frac{a_7^*}{V_7} + \frac{V_7}{a_7^*}\right) \tag{32}$$

The mixture fuel-air ratio is needed for the preceding calculation and is given by

$$f_m = (1 - C)f_B \tag{33}$$

The mixing-zone pressure ratio is then obtained by solving equation (29).

The value of the specific-heat ratio of the mixture corresponds to f_M and T_8'.

Afterburner. - The combustion gas must first be diffused to an afterburner-inlet velocity which permits efficient combustion. The pressure ratio across the afterburner diffuser is given by

$$\frac{p_9'}{p_8'} = \left\{\frac{1 - \frac{\gamma_8 - 1}{\gamma_8 + 1}\left[(1 - \eta_D)\left(\frac{V_8}{a_8^*}\right)^2 + \eta_D\left(\frac{V_{AB}}{a_9^*}\right)^2\right]}{1 - \frac{\gamma_8 - 1}{\gamma_8 + 1}\left(\frac{V_{AB}}{a_9^*}\right)^2}\right\}^{\frac{\gamma_8}{\gamma_8 - 1}} \tag{34}$$

which is obtained from the definition of the afterburner diffuser efficiency. The afterburner pressure ratio depends upon the afterburner-exit critical velocity ratio. On the basis of a constant-area combustion section (assumption (16)) and upon a flame-holder and friction drag loss given by a constant times the inlet dynamic head, the afterburner-exit critical velocity ratio can be obtained from the simultaneous solution of the continuity and momentum relations written across the combustion zone. The solution for the exit critical velocity ratio takes the form

$$\frac{V_{10}}{a^*_{10}} = Z_{10} - \sqrt{Z_{10}^2 - 1} \tag{35}$$

in which

$$Z_{10} = \frac{1}{2}\left[\frac{a^*_9}{V_{AB}} + \frac{1 + \gamma_8(1-C_D)}{\gamma_8+1}\left(\frac{V_{AB}}{a^*_9}\right)\right]\sqrt{\frac{\gamma_8+1}{\gamma_8}\,\frac{\gamma_{10}}{\gamma_{10}+1}\,\frac{T'_9}{T'_{10}}} \tag{36}$$

In the solution of equation (36), the drag coefficient, the afterburner-inlet velocity, and the afterburner-outlet temperature are assigned. The pressure ratio across the afterburner combustion zone is then obtained from the momentum equation in the form

$$\frac{p'_{10}}{p'_9} = \frac{\left[1 - \left(\frac{\gamma_8-1}{\gamma_8+1}\right)\left(\frac{V_{AB}}{a^*_9}\right)^2\right]^{\frac{1}{\gamma_8-1}}}{\left[1 - \left(\frac{\gamma_{10}-1}{\gamma_{10}+1}\right)\left(\frac{V_{10}}{a^*_{10}}\right)^2\right]^{\frac{1}{\gamma_{10}-1}}}\left[\frac{1 + \left(1 - \frac{\gamma_8 C_D}{\gamma_8+1}\right)\left(\frac{V_{AB}}{a^*_9}\right)^2}{1 + \left(\frac{V_{10}}{a^*_{10}}\right)^2}\right] \tag{37}$$

In the preceding equation, the value of the specific-heat ratio at the exit (station 10) corresponds to the afterburner-exit temperature and the afterburner fuel-air ratio given by equation (20) of reference 10.

Cooled-engine performance. - Since the complete expansion of the combustion gas is called for by assumption (18), the unit thrust for either the nonafterburning or the afterburning engine is given by

$$\frac{F}{A_T} = \frac{w_C}{A_T}\left[\frac{(1+f)V_j}{g} - \frac{V_\infty}{g}\right] \tag{38}$$

For the nonafterburning engine,

[redacted]

$$V_j = \sqrt{2gJ\eta_N(h_8' - h_{11})} \tag{39}$$

and

$$f = f_M \tag{40}$$

whereas for the afterburning engine,

$$V_j = \sqrt{2gJ\eta_N(h_{10}' - h_{11})} \tag{41}$$

and

$$f = f_{AB} \tag{42}$$

The values of h_{10}' and h_{11} can be obtained from the charts of reference 10 corresponding to the pertinent state conditions. The value of h_8' is given by equation (28).

The thrust specific fuel consumption is given by

$$sfc_F = \frac{3600fw_C/A_T}{F/A_T} \tag{43}$$

in which f is obtained from either equation (40) or (42), depending on whether F/A_T is for the nonafterburning or the afterburning engine.

Relative component frontal areas. - It is desirable to compare the frontal areas of the several components with the frontal area of the turbine where the engine weight flow is considered limited herein. The ratio of the inlet diffuser frontal area to the turbine frontal area for supersonic flight Mach numbers is given by the following identity:

$$\frac{A_I}{A_T} \equiv \left(\frac{w_C\sqrt{\theta_2}}{A_T\delta_2}\right) \Bigg/ \left(\frac{w_C\sqrt{\theta_2}}{A_I\delta_2}\right) \tag{44}$$

in which the following equations, obtained from the weight-flow balance on compressor and turbine and the continuity relation, respectively, are required:

$$\frac{w_C\sqrt{\theta_2}}{A_T\delta_2} = \frac{w_T}{A_T}\frac{\sqrt{\theta_2}/\delta_2}{(1 + f_B)(1 - C)} \tag{45}$$

and

$$\frac{w_c\sqrt{\theta_2}}{A_I\delta_2} = \frac{p_0 M_\infty \sqrt{\gamma_\infty g/RT_0}}{\eta_R\left(1 + \frac{\gamma_\infty - 1}{2} M_\infty\right)^{\frac{\gamma_\infty + 1}{2(\gamma_\infty - 1)}}} \tag{46}$$

In the case of the compressor, the following two self-evident relations may be employed in conjunction with equation (8) to determine graphically the ratio of the compressor to the turbine frontal areas:

$$\frac{A_C}{A_T} = \left(\frac{U_{C,t}}{U_t}\right)^2 \tag{47}$$

and

$$\frac{w_c\sqrt{\theta_2}}{A_T\delta_2} \equiv \frac{A_C}{A_T}\frac{w_c\sqrt{\theta_2}}{A_C\delta_2} \tag{48}$$

The previous two equations were employed to plot figure 8, from which the ratio of the compressor to turbine frontal area can be obtained for a given turbine tip speed and turbine-limited specific weight flow. In the case of the combustor and the afterburner, the following respective equations derived from the continuity relation give the ratio of either the combustor or afterburner frontal area to that of the turbine:

$$\frac{A_B}{A_T} = \left(\frac{r_{B,h}}{r_t}\right)^2 + \frac{\frac{w_T}{A_T}\frac{RT'_3}{V_B p'_3}}{\left[1 - \frac{\gamma - 1}{\gamma + 1}\left(\frac{GV_B}{a^*_3}\right)^2\right]^{\frac{1}{\gamma - 1}}} \tag{49}$$

$$\frac{A_{AB}}{A_T} = \frac{(1 + f_{AB})w_c/A_T}{\frac{p'_9 a^*_9}{RT'_9}\left(\frac{V_{AB}}{a^*_9}\right)\left[1 - \frac{\gamma_8 - 1}{\gamma_8 + 1}\left(\frac{V_{AB}}{a^*_9}\right)^2\right]^{\frac{1}{\gamma_8 - 1}}} \tag{50}$$

CONCLUDING REMARKS

The relations have been presented from which the design-point performance of both nonafterburning and afterburning turbojet engines

having air-cooled turbines may be determined. In the development, the engine design performance was related to the turbine design specifications of a single-stage turbine in order that the same turbine specifications may be employed to compute the coolant requirements of any cooled-blade configuration. In order to relate the engine performance to the turbine design variables, the specific weight flow and specific work of the turbine were limited by assigning values to certain turbine aerodynamic limits. In addition, in order that the analysis apply to a series of comparable engines, the performance of the several components was also fixed by assigning values to component aerodynamic limits. In the analysis, the coolant-flow ratio was arbitrarily assigned so that the results apply to the use of any air-cooled blade configuration. For the aerodynamically limited turbines, the coolant flow reduces the obtainable compressor pressure ratio, as well as causes losses in stagnation temperature and pressure, in mixing with the combustion gas downstream of the turbine. All these effects are accounted for in the analysis.

Lewis Flight Propulsion Laboratory
National Advisory Committee for Aeronautics
Cleveland, Ohio, April 21, 1954

APPENDIX - SYMBOLS

The following symbols are used in this report:

A	frontal area, sq ft
a^*	critical velocity of sound, $\sqrt{\frac{2\gamma}{\gamma+1} gRT'}$, ft/sec
B	experimental constant in eq. (21)
C	coolant-flow ratio (ratio of coolant weight flow to compressor weight flow)
C_D	drag coefficient
E	experimental constant in eq. (21)
F	thrust, lb
f	fuel-air ratio
fn	function
G	ratio of maximum combustor-inlet flow area to compressor-outlet flow area
g	acceleration due to gravity, ft/sec^2
h	static enthalpy, Btu/lb
h'	stagnation enthalpy, Btu/lb
J	mechanical equivalent of heat, ft-lb/Btu
K_1	constant defined by eq. (14)
K_2	constant defined by eq. (15)
M	Mach number
p_0	NACA standard atmospheric pressure at sea level, 2116 lb/sq ft
p_∞	ambient free-stream pressure, lb/sq ft

p'	stagnation pressure, lb/sq ft
p'_x	absolute stagnation pressure based on axial velocity component, lb/sq ft
R	gas constant, ft-lb/(lb)($^{\circ}$R)
r	radius, ft
S	parameter defined by eq. (23), $\frac{\sec \sqrt{^{\circ}R}}{ft}$
sfc_F	thrust specific fuel consumption, (lb/hr)/lb
T_0	NACA standard atmospheric temperature at sea level, 518.4 $^{\circ}$R
T'	stagnation temperature, $^{\circ}$R
U	blade speed, ft/sec
V	absolute velocity, ft/sec
V_{AB}	afterburner-inlet velocity, ft/sec
V_B	combustor reference velocity, defined as velocity required for combustor to pass its weight flow through the largest flow area at inlet density, ft/sec
V_u	tangential component of absolute velocity, ft/sec
V_x	axial component of absolute velocity, ft/sec
W	velocity relative to rotor, ft/sec
w	weight flow, lb/sec
Z_8	parameter defined by eq. (32)
Z_{10}	parameter defined by eq. (36)
α	angle between tangential direction and absolute efflux velocity of turbine, deg

[redacted]

γ	without subscript 4/3, ratio of specific heat; with subscript, a function of local stagnation temperature and fuel-air ratio
$\Delta h'_C$	specific compressor work, Btu/lb
$\Delta h'_T$	specific turbine work, Btu/lb
δ	ratio of stagnation to standard pressure, p'/p_0
η	adiabatic efficiency
η_D	diffuser efficiency
η_N	nozzle efficiency
η_R	ram recovery
θ	ratio of stagnation to standard temperature, T'/T_0

3308

Subscripts:

AB	afterburner
B	combustor
C	compressor
h	hub or inner radius (refers to turbine hub when used alone as subscript)
I	inlet diffuser
i	integrated mean
j	jet
M	mixture
m	mean radial position
R	relative (except when used with η)
T	turbine
t	tip (refers to turbine tip when used alone as subscript)

[redacted]

1 to 11 engine stations as shown on fig. 1

- ambient free stream

REFERENCES

1. Rossbach, Richard J., Schramm, Wilson B., and Hubbartt, James E.: Analysis of Factors Affecting Selection and Design of Air-Cooled Single-Stage Turbines for Turbojet Engines. I - Turbine Performance and Engine Weight-Flow Capacity. NACA RM E54C22, 1954.

2. Arne, Vernon L., and Nachtigall, Alfred J.: Calculated Effects of Turbine Rotor-Blade Cooling-Air Flow, Altitude, and Compressor Bleed Point on Performance of a Turbojet Engine. NACA RM E51E24, 1951.

3. Ziemer, Robert R., Schafer, Louis J., Jr., and Heaton, Thomas R.: Performance of Two Air-Cooled Turbojet Engines Determined Analytically from Engine Component Performance for a Range of Cooling-Air Weight Flows. NACA RM E53K19, 1954.

4. Cavicchi, Richard H., and English, Robert E.: A Rapid Method for Use in Design of Turbines within Specified Aerodynamic Limits. NACA TN 2905, 1953.

5. Wu, Chung-Hua, and Wolfenstein, Lincoln: Application of Radial-Equilibrium Condition to Axial-Flow-Compressor and Turbine Design. NACA Rep. 955, 1950. (Supersedes NACA TN 1795.)

6. Ainley, D. G.: An Experimental Single-Stage Air-Cooled Turbine. Pt. II - Research on the Performance of a Type of Internally-Air-Cooled Turbine Blade. Aircraft Eng., vol. XXV, no. 295, Sept. 1953, pp. 269-276.

7. Zettle, Eugene V., and Cook, William P.: Performance Investigation of Can-Type Combustor. I - Instrumentation, Altitude Operational Limits, and Combustion Efficiency. NACA RM E8F17, 1948. (Supersedes NACA RM E6L05.)

8. Bohanon, H. R., and Wilcox, E. C.: Theoretical Investigation of Thrust Augmentation of Turbojet Engines by Tail-Pipe Burning. NACA RM E6L02, 1947.

9. Durham, F. P.: Increased Jet Thrust from Pressure Forces. Jour. Aero. Sci., vol. 17, no. 7, July 1950, pp. 425-428.

10. English, Robert E., and Wachtl, William W.: Charts of Thermodynamic Properties of Air and Combustion Products from 300° to 3500° R. NACA TN 2071, 1950.

[redacted]

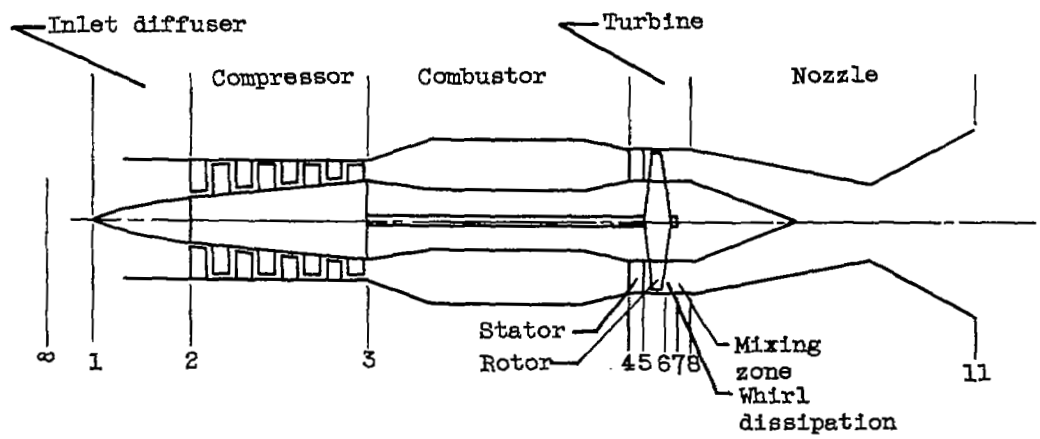

(a) Nonafterburning engine.

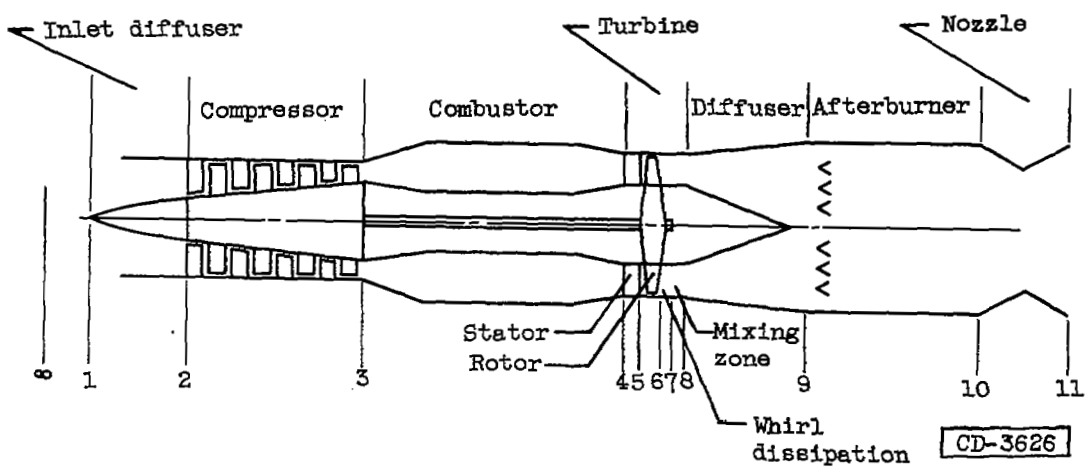

(b) Afterburning engine.

Figure 1. - Schematic diagram of two turbojet engines.

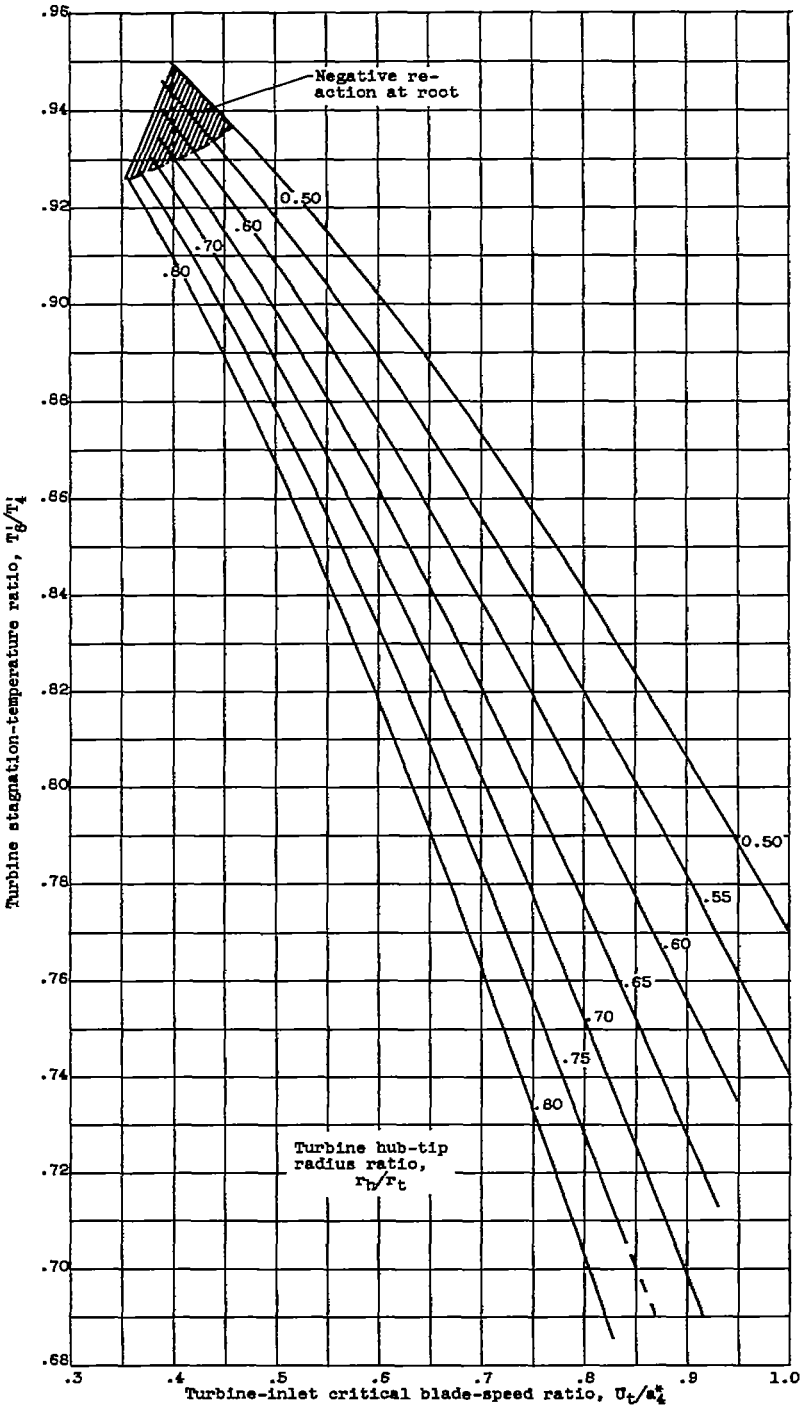

Figure 2. - Variation of aerodynamically limited turbine temperature ratio with inlet critical blade-speed ratio and turbine hub-tip radius ratio. Inlet relative Mach number at hub, 0.8; exit axial critical velocity ratio, 0.7; integrated mean exit whirl parameter $V_{u,6,i}/U_1$, -0.41; adiabatic efficiency, 0.85.

[redacted]

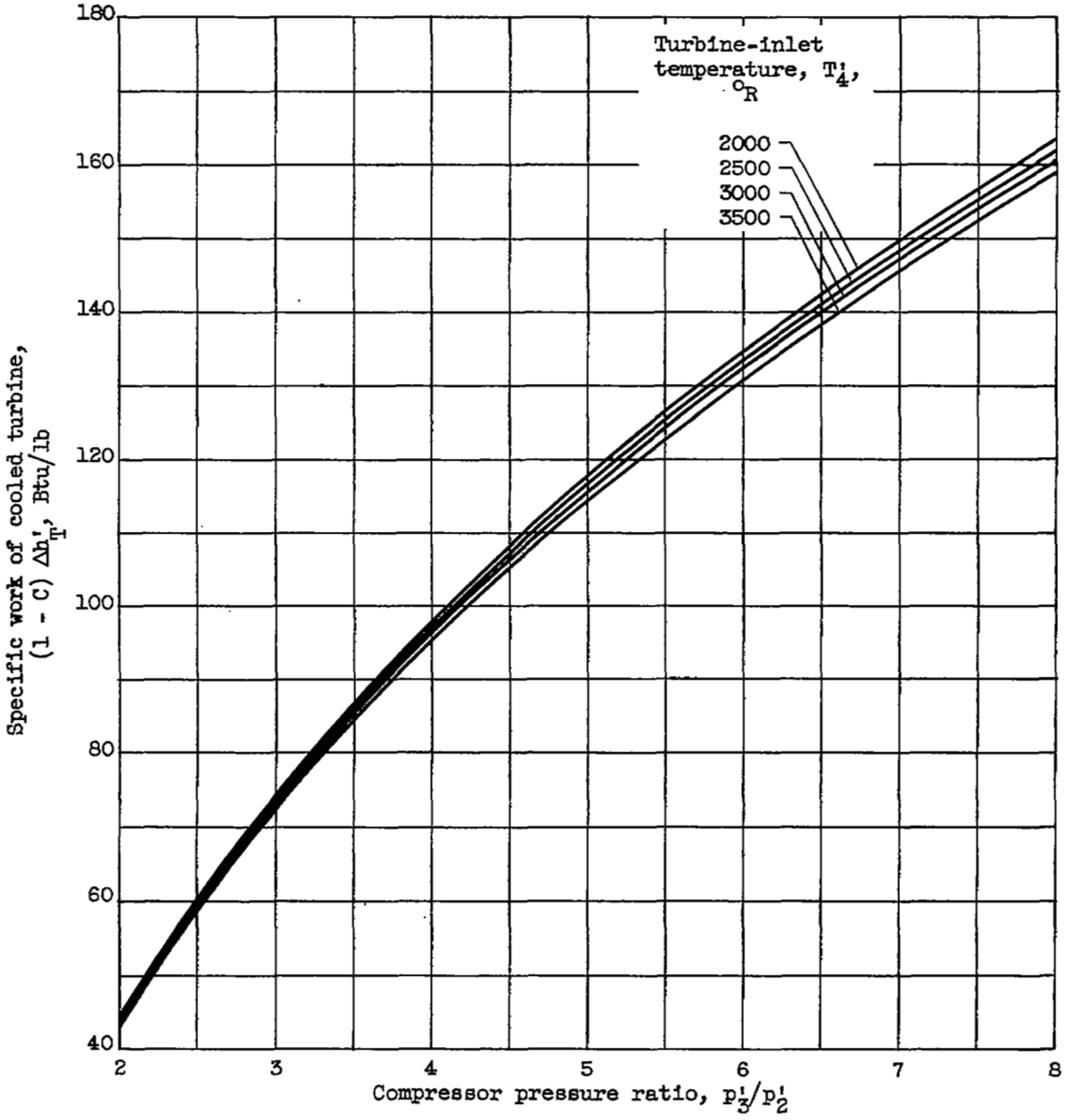

Figure 3. - Variation of specific work of cooled turbine with compressor pressure ratio and turbine-inlet temperature. Compressor-inlet temperature, 708° R; adiabatic efficiency, 0.83.

[redacted]

3308

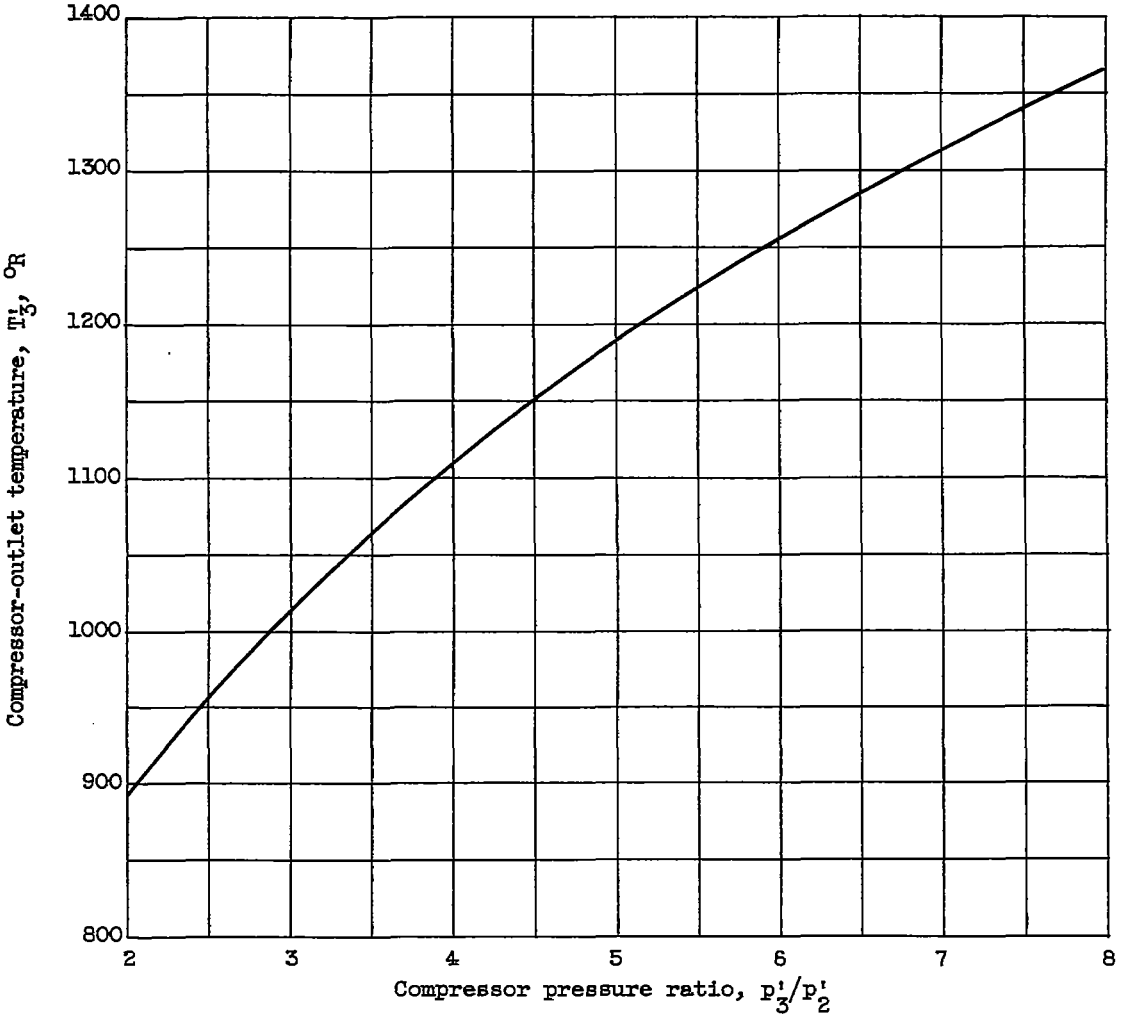

Figure 4. - Variation of compressor-outlet temperature with pressure ratio. Compressor-inlet temperature, 708° R; adiabatic efficiency, 0.83.

[redacted]

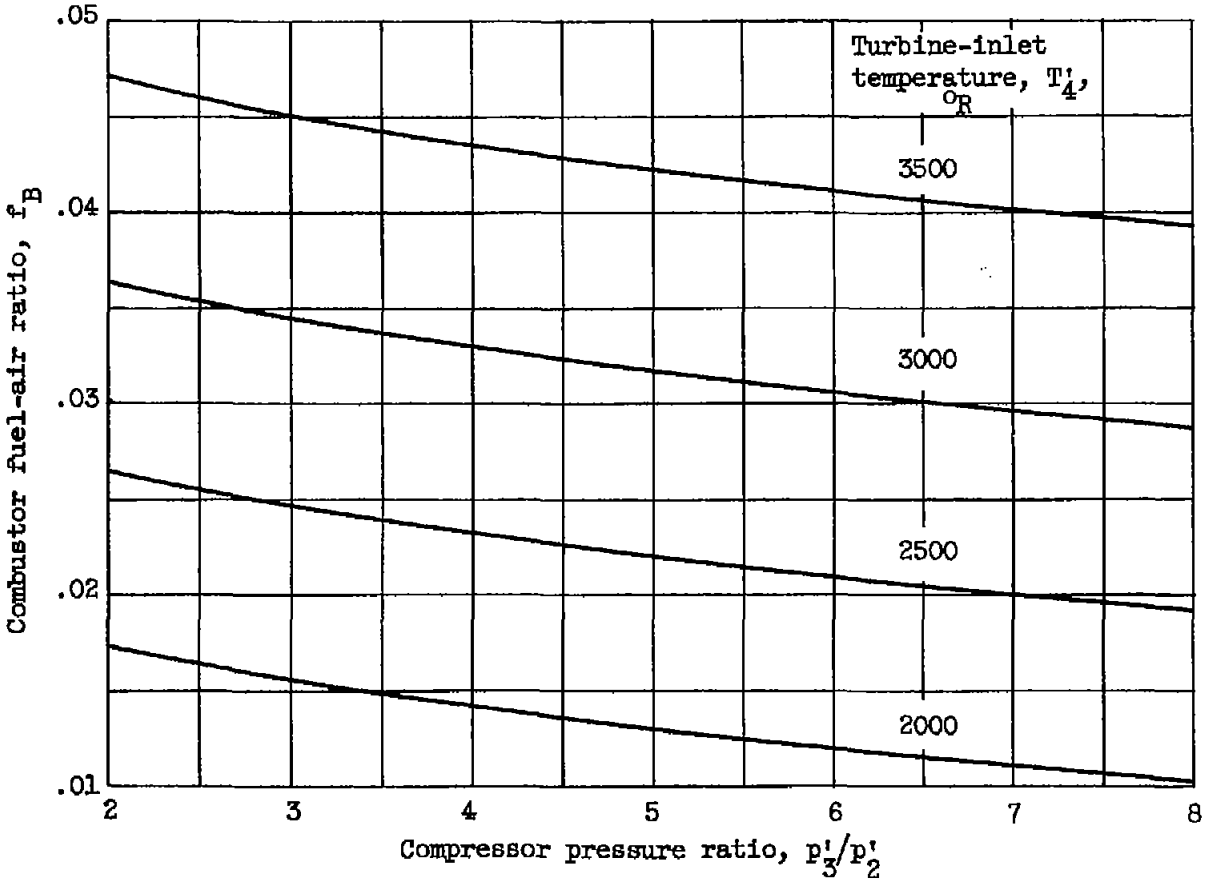

Figure 5. - Variation of fuel-air ratio with compressor pressure ratio and turbine-inlet temperature. Compressor-inlet temperature, 708° R; adiabatic efficiency, 0.83.

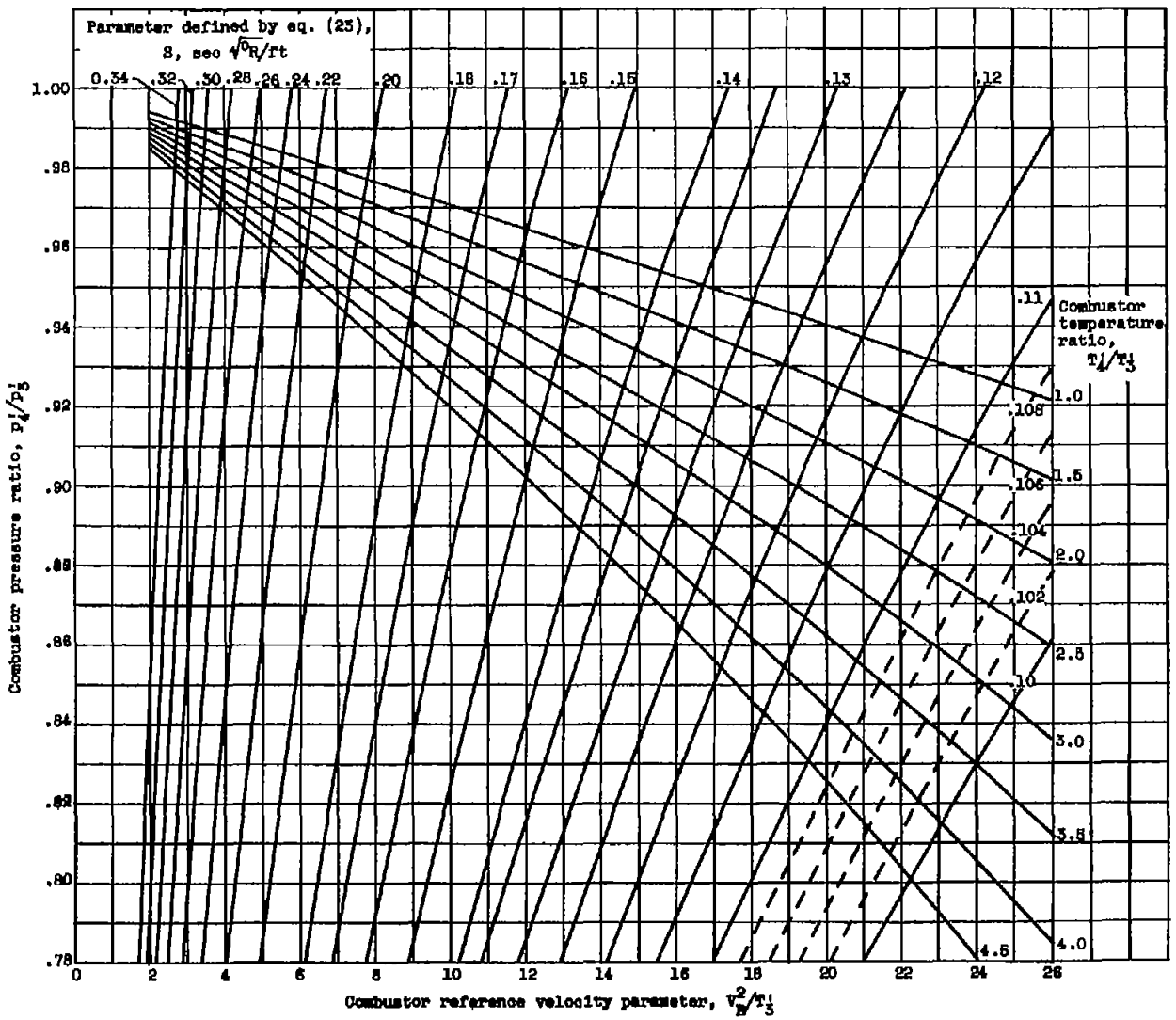

Figure 6. - Simultaneous solutions of combustor pressure ratio relations. (Pressure-drop characteristics of ref. 7 used.) Combustor diffuser area ratio, 3.0; ratio of combustor inner radius to turbine outer radius, 0.25.

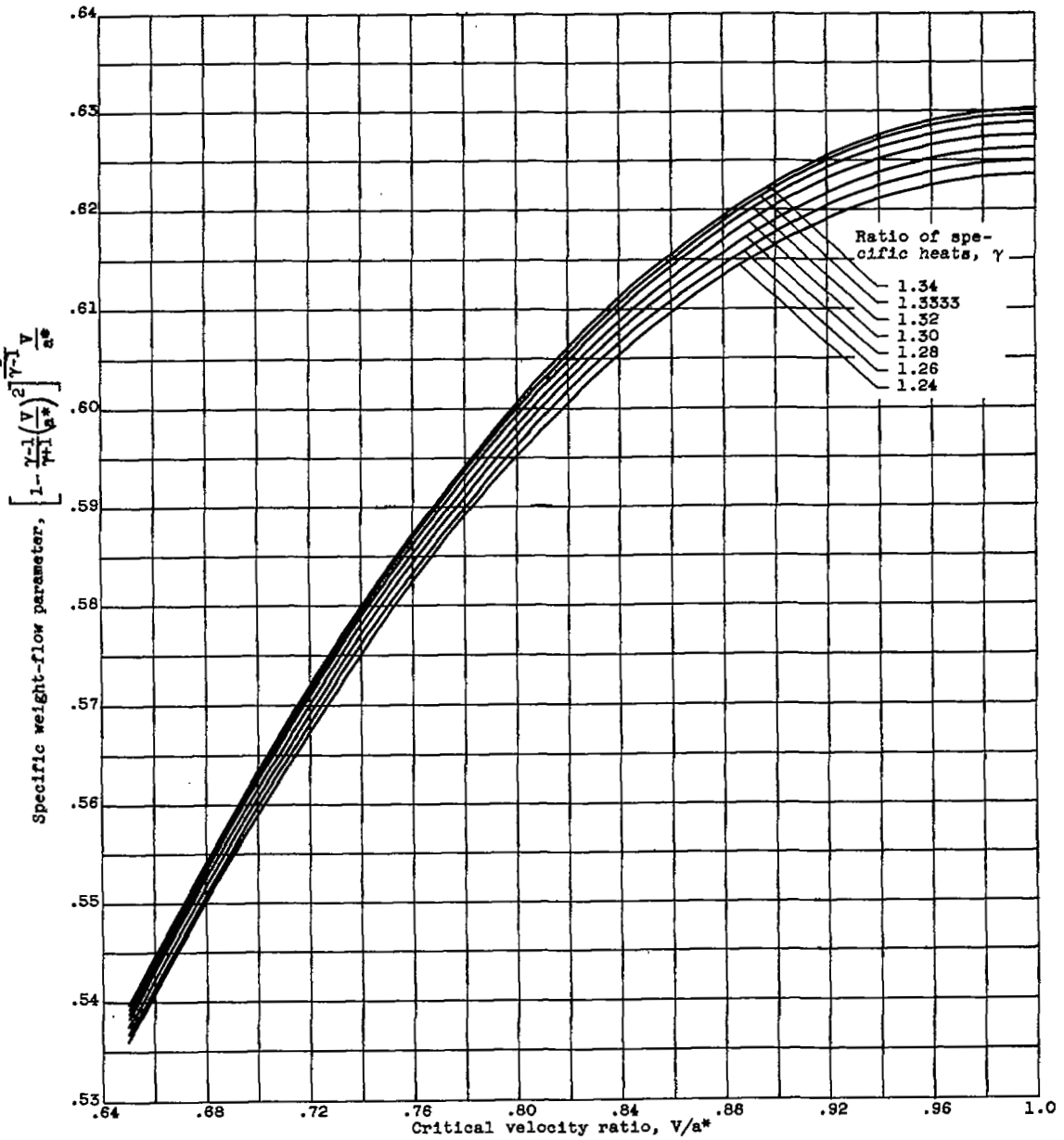

Figure 7. - Variation of specific weight-flow parameter with critical velocity ratio. Zero tangential velocity.

3308

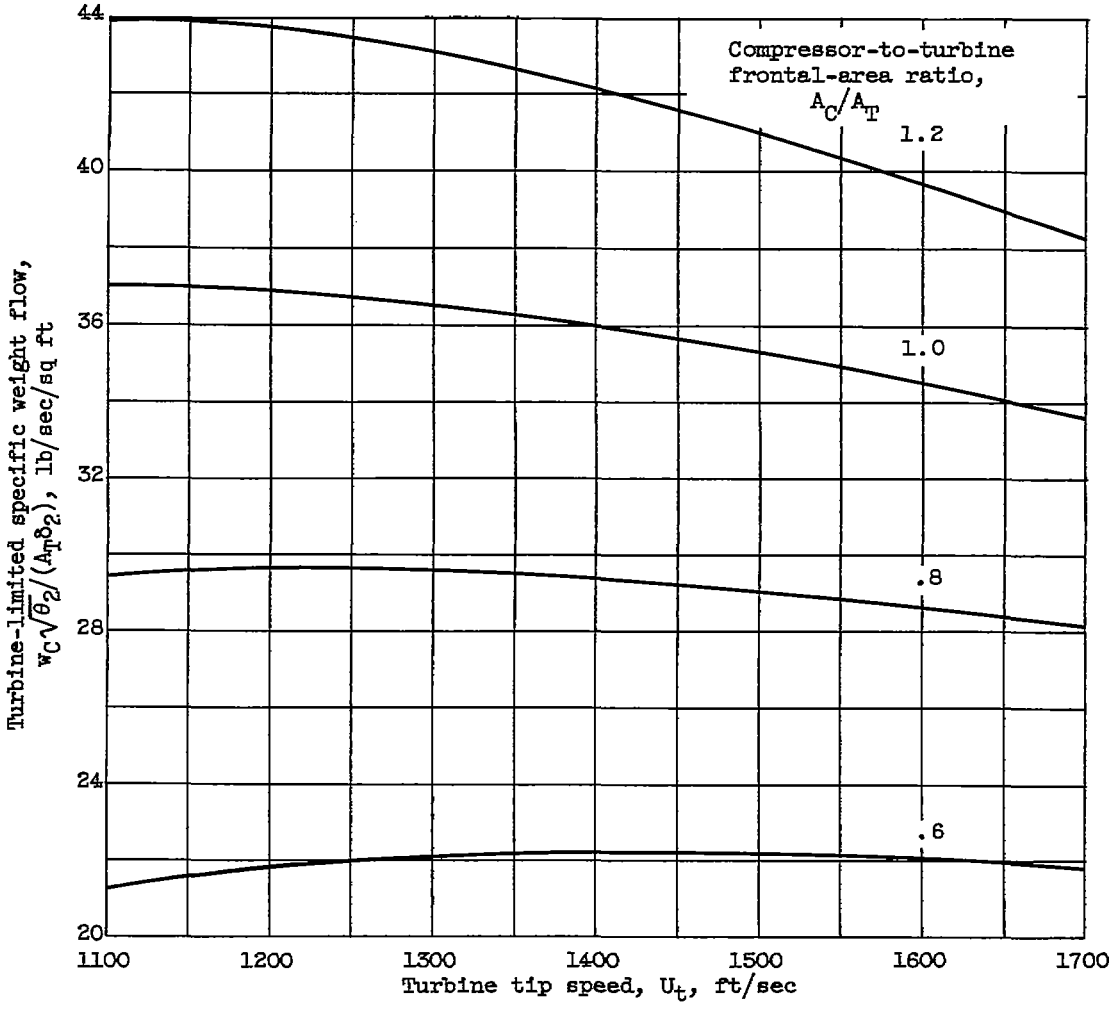

Figure 8. - Comparative frontal areas of matching compressor and turbine. Compressor-rotor-inlet relative Mach number, 1.1; compressor-inlet axial critical velocity ratio at hub, $V_{x,2,h}/a_2^*$, 0.7.

NACA-Langley - 6-21-54 - 350